THE JOURNAL OF BIOLOGICAL CHEMISTRY
Vol. 274, No. 7, Issue of February 12, pp. 4220–4224, 1999
Printed in U.S.A.

Crystal Structure of Neuropsin, a Hippocampal Protease Involved in Kindling Epileptogenesis*

(Received for publication, September 11, 1998)

Tadaaki Kishi‡, Masato Kato‡, Toshiyuki Shimizu, Keiko Kato§, Kazumasa Matsumoto§, Shigetaka Yoshida§, Sadao Shiosaka§, and Toshio Hakoshima¶

From the Department of Molecular Biology and the §Department of Cell Biology, Nara Institute of Science and Technology, 8916-5 Takayama, Ikoma, Nara 630-0101, Japan

Neuropsin is a novel serine protease, the expression of which is highly localized in the limbic areas of the mouse brain and which is suggested to be involved in kindling epileptogenesis and hippocampal plasticity. The 2.1-Å resolution crystal structure of neuropsin provides the first three-dimensional view of one of the serine proteases highly expressed in the nervous system, and reveals a serine protease fold that exhibits chimeric features between trypsin and nerve growth factor-γ (NGFγ), a member of the kallikrein family. Neuropsin possesses an *N*-glycosylated "kallikrein loop" but forms six disulfide bonds corresponding to those of trypsin. The ordered kallikrein loop projects proline toward the active site to restrict smaller residues or proline at the P2 position of substrates. Loop F, which participates in forming the S3/S4 sites, is similar to trypsin rather than NGFγ. The unique conformations of loops G and H form an S1 pocket specific for both arginine and lysine. These characteristic loop structures forming the substrate-binding site suggest the novel substrate specificity of neuropsin and give a clue to the design of its specific inhibitors.

Proteases have been shown to play essential roles in the nervous system, including those of neurite outgrowth (1), neural degeneration (2), and synaptic plasticity (3). These actions are thought to be mediated by the proteolytic cleavage of zymogen precursors, the activation of specific cell surface receptors, or the degradation of extracellular matrix proteins (4). Neuropsin was cloned from a mouse hippocampal cDNA library using sequences for key regions of the serine protease domain of nerve growth factor (NGF)-γ[1] (5). In the brain, no NGFγ has been identified so far, though NGFβ is present. Neuropsin is one of the serine proteases highly expressed in the nervous system (6–8). The expression of neuropsin is localized at highest concentration in the hippocampus and the amygdala, which are important for acquisition of memory and emotional memory, respectively. This localization is in contrast to that of tissue plasminogen activator (tPA), which is well documented to play a crucial role in the nervous system by mediating plasticity but is distributed more uniformly across the other brain regions and throughout other organs (9). Activity-dependent changes in expression of neuropsin have been observed upon direct hippocampal stimulation and induction of kindling, which is a model for epilepsy and neuronal plasticity characterized by the progressive development of electrographic and behavioral seizures (5, 10). A single intraventricular injection of monoclonal antibodies specific to neuropsin reduces or eliminates the epileptic pattern (11). Moreover, oxidative stress is shown to effect the expression of neuropsin in the limbic areas, which might be related to the disturbance in shock-avoidance learning of mice (12). These activity-dependent changes and the specific localization of neuropsin indicate the involvement of this protease in hippocampal plasticity and its pathogenesis. Knowledge of the three-dimensional structure of neuropsin provides clues to the biological activity of this protease and also is important to the design of inhibitors that might be useful in treatment of pathological conditions such as epilepsy.

EXPERIMENTAL PROCEDURES

Protein Preparation and Crystallization—Neuropsin was over-expressed in baculovirus-infected High Five insect cells, purified, and crystallized as described previously (13). The resulting sample and the crystallized protein were verified with N-terminal analysis using an Applied Biosystem automatic analyzer 476A. Neuropsin has a putative glycosylation site at Asn^{95} of the kallikrein loop. Time-of-flight mass spectroscopy with PerSeptive JMS-ELITE matrix-associated laser desorption/ionization time-of-flight indicated its heterogeneous glycosylation. Two-dimensional high performance liquid chromatography mapping (14) revealed that the *N*-glycans contained 89% paucimannosidic structures with and without attached fucose residue(s) at the innermost GlcNAc residues but the glycosylation pattern exhibited high heterogeneity as found on many glycoproteins (15). The detailed procedures and obtained structures will be described elsewhere. The crystals belong to space group $P1$ (a = 38.15 Å, b = 54.95 Å, c = 64.29 Å, α = 95.72°, β = 90.03°, and γ = 110.29°). X-ray diffraction data were collected with Rigaku imaging plate area-detectors, R-Axis IV and R-Axis IIc, using Cu-K_α radiation and also with a Weissenberg camera at the BL-18B beamline station of the Photon Factory, Tsukuba using 1-Å radiation. Intensities were evaluated with the program DENZO/SCALEPAK (16), which yielded 25,778 independent combined reflections corresponding to 90.7% completeness at 2.1-Å resolution (74.5% in the highest resolution bin), an R_{merge} of 6.0% (19.8%), a mean ratio of intensity, and σ of 8.5 (3.1).

Structure Determination—Initial phases were calculated by molecular-replacement with the program AMoRe (17) using a search model based on the structure of bovine pancreatic β-trypsin (PDB code 4PTP) (18). Rigid body refinements of the searched model were performed with the program X-PLOR (19), followed by density averaging/histogram

* This work was supported by Grants-in-Aid for Scientific Research (09308025, 10359003), on Priority Areas (10179104, 09277102), Biometalics (09235220) (to T. H.) from the Ministry of Education, Science, Sports and Culture, Japan. The costs of publication of this article were defrayed in part by the payment of page charges. This article must therefore be hereby marked "*advertisement*" in accordance with 18 U.S.C. Section 1734 solely to indicate this fact.

The atomic coordinates and structure factors (code 1NPM) have been deposited in the Protein Data Bank, Brookhaven National Laboratory, Upton, NY.

‡Supported by a research fellowship for young scientists from the Japan Society for the Promotion of Science.

¶ A member of the TARA project of Tsukuba University. To whom correspondence should be addressed. Tel.: 0743-72-5570; Fax: 0743-72-5579; E-mail: hakosima@bs.aist-nara.ac.jp.

[1] The abbreviations used are: NGF, nerve growth factor; tPA, tissue plasminogen activator; GlcNAc, *N*-acetylglucosamine; STI, soybean trypsin inhibitor; MCA, 4-methylcoumaryl-7-amide; MSP, myelencephalon-specific protease; r.m.s., root mean square.

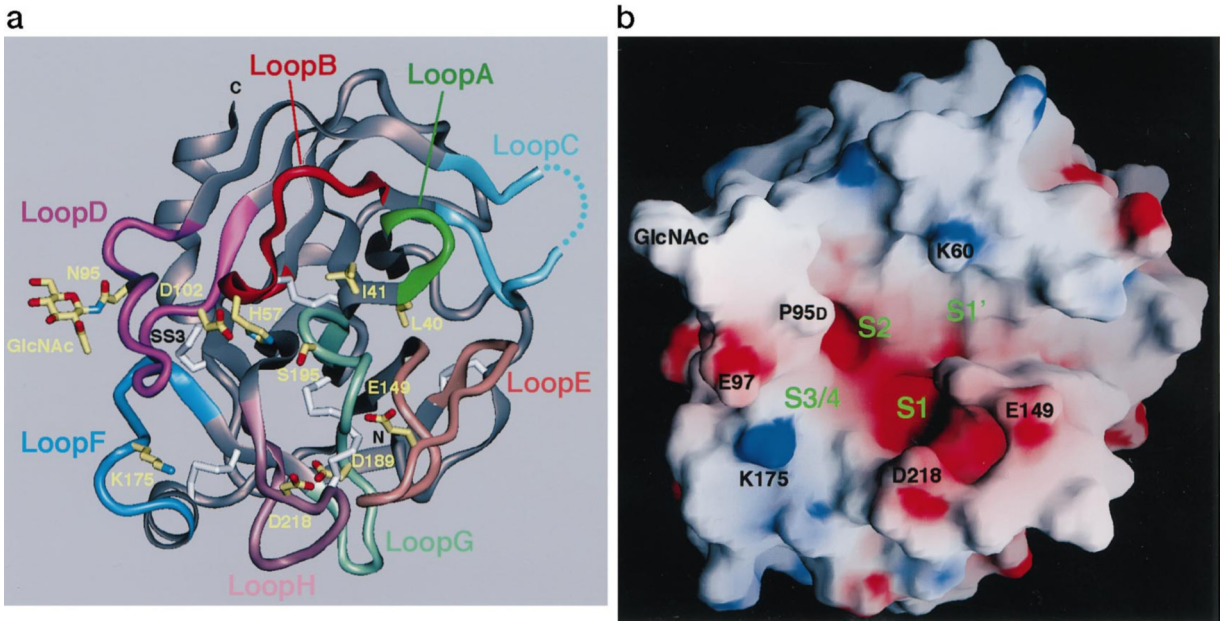

FIG. 1. **Overall structure of neuropsin.** *a*, ribbon representation of neuropsin. Seven-stranded β-sheets (the top and bottom halves) are sandwiched with the catalytic triad at the cleft of the β-sandwich. The surface loops (*A–H*) forming the substrate-binding site are *colored* with labels. Six disulfide bonds are shown by bridges in *white,* and the disulfide bond (*SS3*), which is conserved in trypsin but not in kallikrein, was labeled. *Loop D* is the kallikrein loop that has an *N*-glycosylated Asn^{95} with one visible GlcNAc residue. The side chains of the catalytic triad, Asp^{189} at the S1-specific pocket, Lys^{175} at the S3/4 site, Glu^{149} and Asp^{218} at the rim of the S1 pocket, and Leu^{40} and Ile^{41} at the S1′ site, are also shown with *stick* representations with one-letter amino acid labels. *b*, molecular surfaces of neuropsin viewed from nearly the same direction of *panel a*. Surface electrostatic potentials calculated and rendered using GRASP (negative potentials are in *red* and positive in *blue*). The S1–S4 and S1′ sites and characteristic surface residues are labeled.

matching with the program DM (20). Six regions of insertions and deletions were inspected on the resulting $2F_o - F_c$ map, which was generated with the program O (21). The structure was built and refined through alternating cycles using the programs O and X-PLOR, respectively. The kallikrein loop had large but mostly poor density connects to the side chain of Asn^{95}. After several cycles of refinements incorporating solvent water molecules located at the regions other than the kallikrein loop, we defined one residue of *N*-acetylglucosamine (GlcNAc) residue bonded to Asn^{95}, as well as weaker density for additional sugar residues that we have been unable to identify definitively. The residual weak density is extending toward a large solvent channel in the crystal.

Current Structure—Two regions were poorly defined in the map. The first is at the loop residues, Arg^{74} and Asp^{75}, and the second is at the three C-terminal residues. These have uninterpretable densities implying complex disorder. The current structure contains 194 water molecules. The R-factor is 18.6% (an R_{free} of 22.7%) for all reflections to 2.1-Å resolution. The root-mean-square (r.m.s.) deviations from target values are 0.008 Å for bond lengths, 1.535° for bond angles, and 1.139° for the peptide torsion angles. The averaged B-factor is 30.8 $Å^2$. There is no residue in disallowed regions as defined in PROCHECK (22), but 89.4% residues in the most favorable regions and 10.6% residues in the additional allowed regions.

RESULTS

Overall Structure—Neuropsin consists of fourteen β-strands (designated as β1–β14) that are extensively twisted, two α-helices (designated as α1 and α2), and one short 3_{10}-helix (Fig. 1*a*). Each seven-β-strand forms an antiparallel β-sheet folded in a β-sandwich with a cleft where the catalytic triad (Asp^{57}, His^{102}, and Ser^{195}) is located (Fig. 1, *a* and *b*). This overall structure is homologous to those of the chymotrypsin-type serine proteases, which share an identical catalytic mechanism, but among which the substrate specificity varies. Many known structures of these proteases delineate a clear framework, demonstrating that this variety is a function of evolved diversity in the structures of surface loops that surround the substrate-binding site. Because the loops of neuropsin, which contains eight prominent loops (*A–H* in Fig. 1*a*), are conserved in their relative positions with respect to the active site, general themes for their individual functions can be derived.

One of the characteristic features of neuropsin is the *N*-glycosylated loop D that corresponds to the so-called "kallikrein loop." This loop, having an Asn-*X*-Ser sequence, is typical for members of the kallikrein family that contains NGFγ, which exhibits relatively high (46%) sequence identity to neuropsin (Fig. 2). Neuropsin, however, forms six disulfide bonds corresponding to those of trypsin with an additional disulfide bond (SS3 between Cys^{128} and Cys^{232} in Fig. 1*a*) that is missing in members of the kallikrein family. Large differences exist in the loop regions surrounding the substrate-binding site, whereas the core region contains only minor variations. Excluding the insertion and deletion residues, the main-chain atoms of neuropsin superimpose on the corresponding atoms of bovine pancreatic trypsin (18), mouse submaxillary gland NGFγ in 7 S NGF (23), an $\alpha_2\beta_2\gamma_2$ complex of NGF, and pancreatic porcine kallikrein (24) with r.m.s. deviations of 1.26, 1.43, and 1.84 Å, respectively. The geometry of the catalytic triad is highly similar to those of the serine proteases with r.m.s. deviations in a range of 0.2–0.24 Å. Neuropsin has no prominent structural similarity to tPA, showing a high r.m.s. deviation of 2.74 Å for 79 identical residues (37% sequence identity).

S1 Site—Enzyme assay using several 4-methylcoumaryl-7-amide (MCA) derivatives of oligopeptides (25) has shown that neuropsin cleaves peptide bonds C-terminal to Arg or Lys. This primary specificity is well interpreted by the S1 pocket, a deep cylindrical pocket that is formed by two loops, G and H, and punctuated at its base by the side chain of Asp^{189}. However, neuropsin has large conformational changes of loop G with maximum displacements of 4.8–5.8 Å compared with those of NGFγ, kallikrein, and trypsin (Fig. 3). The conformational changes in neuropsin seem to be caused by the one-residue (Gly^{186B}) deletion in loop G. In addition, loop H of neuropsin also displays large displacements from these proteases because

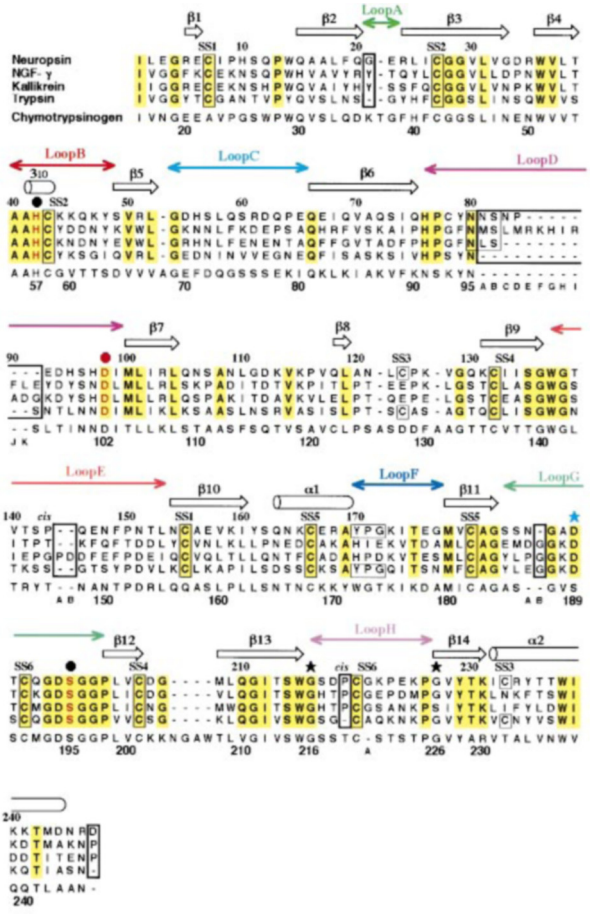

FIG. 2. **Secondary structural elements and sequence alignment of neuropsin and the related proteases, mouse submaxillary gland NGFγ, porcine pancreatic kallikrein A, and bovine pancreatic β-trypsin.** The sequential numbering of neuropsin is shown at the *top*, and the chymotrypsinogen based used throughout this paper is at the *bottom*. The secondary structural elements of neuropsin are shown at the *top* with *arrows* for β-strands (*β1–β14*), cylinders for α-helices (*α1*, *α2*), and 3_{10}-helix. The loops (*A–H*) forming the substrate-binding site are marked with *colored bars* with labels. Insertion or deletion sites are marked by *heavy line boxes*. The disulfide-bond-forming cysteines are *boxed* and marked by labels (*SS1–SS6*), which correspond to six disulfide-bonds, respectively. The catalytic triad is marked by *red circles*. Asp^{189} in the S1-specific pocket is marked by a *blue star*. Gly^{216} and Gly^{226} of the rim of the S1 pocket are marked by *black stars*. The putative *N*-glycosylation sequence of Asn-*X*-Ser, which is conserved in members of the kallikrein family, two *cis* prolines of neuropsin, Pro^{147} and Pro^{219}, and Tyr^{172}-Pro^{173}-Gly^{174} of loop F are *boxed*.

loop H is heavily interacted with loop G in all the proteases. It is noteworthy that loop H of trypsin has a one-residue deletion of the *cis* proline, Pro^{219}, that is conserved in neuropsin, NGFγ, and kallikrein. This deletion induces a larger displacement of neuropsin loop H from trypsin (4.3 Å) than from NGFγ (3.4 Å) or kallikrein (3.2 Å). Interestingly, the P1 specificity of neuropsin for arginine is comparable with that for lysine. This is in sharp contrast to NGFγ, kallikrein, and trypsin, in which a significant preference for arginine exists. Among key residues of the S1 pocket, Gly^{226} of neuropsin has relatively large displacements from NGFγ (0.7 Å) and kallikrein (1.2 Å). Alternatively, Ser^{217} of neuropsin has a relatively large displacement from trypsin (1.3 Å). Compared with NGFγ, the changes of the neuropsin loop structures result in positional displacements (0.4–0.8 Å) of Asp^{189}, Thr^{190}, and His^{217}, which have been reported to form hydrogen bonds to the P1 arginine of NGFβ in 7 S NGF (23). These local differences may be responsible for the unique P1 specificity of neuropsin. Like other serine proteases, which are activated by cleavage of the bond between Arg^{15} and Ile^{16}, neuropsin tucks the newly formed amino group of Ile^{16} into the pocket to form multiple hydrogen bonds with the main chains of loop E and to form an ion pair with Asp^{194} of loop G.

Kallikrein Loop—The kallikrein loop of neuropsin differs radically from those of NGFγ and kallikrein. In these members of the kallikrein family, the loop was cleaved into the highly mobile nicked chains. In contrast, the loop of neuropsin is packed into an ordered and relatively compact conformation without any nicked site: neuropsin has no arginine or lysine residue in the loop. Recently determined crystal structure (26) of mouse glandular kallikrein-13 shows an ordered kallikrein loop, but no conformational similarity with the loop of neuropsin. It seems unlikely that the *N*-glycan bound to Asn^{95} participates directly in the substrate binding because the GlcNAc residue and the residual density are oriented away from the active site as in members of the kallikrein family.

S2 Site—The kallikrein loop of neuropsin overhangs toward the active site cleft with a prominent Pro^{95D} residue, which suggests its role in substrate binding. Interestingly, superposition of neuropsin on porcine pancreatic trypsin complexed with soybean trypsin inhibitor (STI) (27) revealed steric clashes between the kallikrein loop of neuropsin and the two STI loops facing toward neuropsin. This was borne out by biochemical experiments in which high molecular weight inhibitors, such as STI or α-antitrypsin, were found to have little effect on the neuropsin activity, whereas low molecular weight inhibitors, such as leupeptin, markedly inhibited the activity. The overhanging kallikrein loop forms a narrow pocket (the S2 site) in which Asp^{102} is positioned at the base and would restrict the size of the side chain in the P2 position of substrate peptides. This is consistent with the results of a previous enzyme assay (25), in which high activities of neuropsin were observed for peptide substrates having smaller residues or proline in the P2 positions. It has been well demonstrated by the crystal structure of thrombin complexed with D-Phe-Pro-Arg that loop B of thrombin compresses the S2 site with the inserted residues, Tyr^{60A} and Trp^{60D}, to deduce the P2 specificity of the enzyme for proline (28). Superposition of neuropsin on thrombin shows Pro^{95D} of neuropsin located nearby Tyr^{60A} and Trp^{60D} of thrombin, but no contact between Pro^{95D} and the proline residue of D-Phe-Pro-Arg bound to thrombin, which suggests that the P2 preference for proline may be mediated by the kallikrein loop of neuropsin, instead of loop B of thrombin, but rather weaker than that of thrombin (Fig. 4). Phenylalanine at the P2 position remarkably reduces the neuropsin activity, which is one of the major differences from kallikrein and NGFγ.

S3/S4 Site—Most striking is the structure of loop F that is similar to that of trypsin rather than NGFγ and kallikrein, where significant conformational changes of loop F from neuropsin occur with large displacements, 5.2 and 6 Å, respectively, accompanied by movements of helix α1 (Fig. 3). Loop F is one of the main elements forming the S3/S4 site. It is notable that this loop has Tyr^{172}, which forms hydrogen bonds with the main chains of loop H and which is conserved in trypsin but is replaced by histidine in NGFγ and kallikrein. This residue has been elucidated to be one of the distal determinant residues for the substrate specificity (29). Moreover, Gly^{174}, which is conserved in neuropsin and trypsin, is one of the key residues for the loop F structure because this residue is an essential component of the type-II reverse turn, YPGK at 172–175. It should be pointed out that the disulfide bond SS3, which is conserved in trypsin as already mentioned, may contribute to the conformational resemblance of loop F with that of trypsin through contacts with strand β13 that associated with the C-terminal β-strand of loop F, β11.

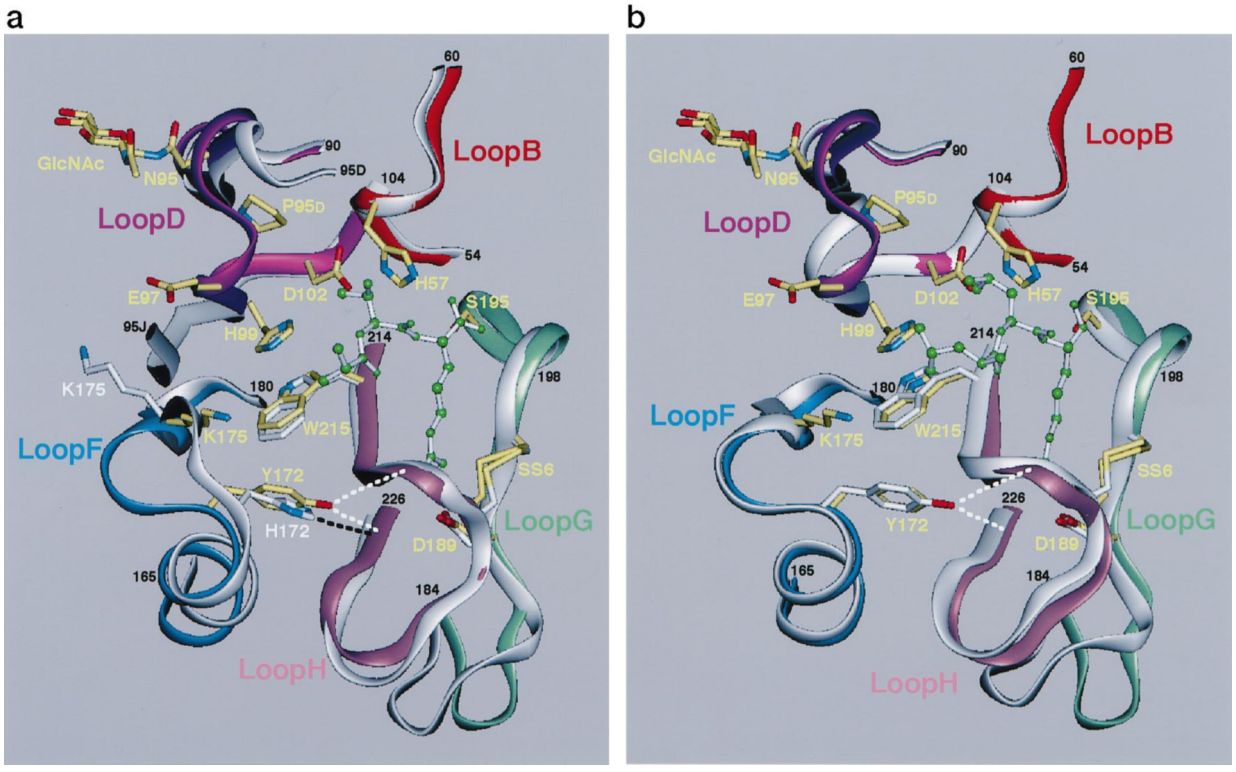

FIG. 3. **Comparison of the surface loops forming the substrate-binding site between neuropsin (*colored*) and the related proteases (*gray*): NGFγ-NGFβ in 7 S NGF (*a*) and trypsin-leupeptin complexes (*b*).** The C_α-carbon atom tracings of loops B, D, and F–H of neuropsin are *colored* as in Fig. 1*a* with both the N- and C-terminal residue numbers in *black* and superimposed on those of the proteases with the bound substrate or inhibitor (*green*); the C-terminal Ala-Thr-Arg of NGFβ in *panel a*, or leupeptin in *panel b*. The side chains of the key residues of the loops and the catalytic triad of neuropsin are shown with *yellow* labels, but the others are not shown for the clarity. Some of the side chains and the disulfide bond SS6 of NGFγ and trypsin are also shown with *white* labels. These are Trp^{215}, His^{172}, Lys^{175}, Asp^{189}, and the disulfide bond SS6 of NGFγ in *panel a*, and Trp^{215}, Tyr^{172}, Asp^{189}, and the disulfide bond SS6 of trypsin. The hydrogen bonds between Tyr^{172} (His^{172} of NGFγ) and loop H are indicated by *white* (*black* for His^{172}) *broken lines*.

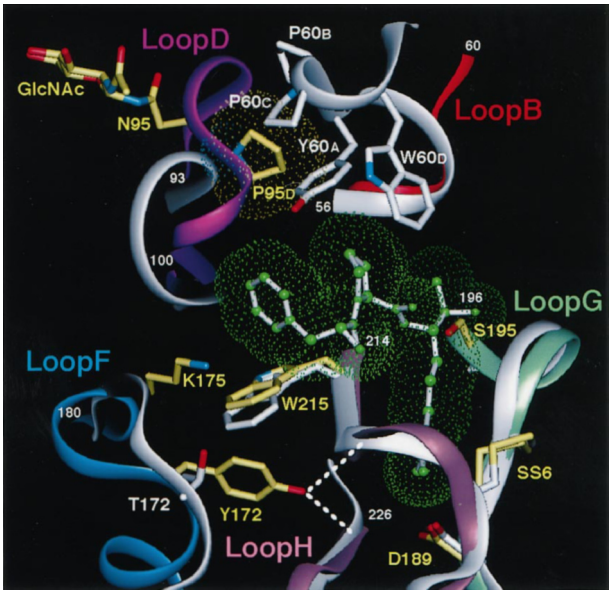

FIG. 4. **Comparison of the surface loops forming the S2 site between neuropsin (*colored*) and α-thrombin (*gray*).** The C_α-carbon atom tracings of loops of neuropsin, colored as in Fig. 1*a*, are superimposed on α-thrombin complexed with D-Phe-Pro-Arg-chloromethylketone (*green*). The van der Waals surfaces of the inhibitor peptide and P95D are shown with *dot-surface* representations. Labels are as in Fig. 3.

It is remarkable that the above differences in the loop F may also be correlated with the conformational differences in the kallikrein loops. In NGFγ and kallikrein, the highly mobile kallikrein loops heavily interact with loop F although the kallikrein loop of neuropsin has no direct interaction with loop F, as it does with loop D of trypsin. One of the interesting consequences of these conformational characteristics in loops D and F is that the S3/S4 site of neuropsin is similar to that of trypsin rather than NGFγ. The aromatic rings of Trp^{215}, Tyr^{172}, and His^{99} provide a shallow but wide hydrophobic depression for the S3/S4 site as in trypsin and could explain the high activities of neuropsin observed for synthetic tripeptide substrates having hydrophobic residues in the P3 position. Moreover, in neuropsin, Lys^{175} of loop F is projected toward the S3/S4 site (Fig. 1*b*), whereas Lys^{175} of NGFγ is projected away from the S3/S4 site. It is interesting that Lys^{175} may play a role in the P3/P4 interaction with the substrates. Actually, one of the cleavage sites of fibronectin (25), which is an extracellular matrix protein exhibiting strong proteolytic sensitivity for neuropsin, had the N-terminal sequence of Asp-Val-Arg, whose acidic residue at the P3 position may interact with Lys^{175}.

DISCUSSION

A tripeptide substrate preferred for thrombin, Val-Pro-Arg-MCA, has been found to exhibit the highest sensitivity for neuropsin to date. However, poor structural homology between neuropsin and thrombin is evident from the large r.m.s. deviation of 2.7 Å for 78 identical residues. Moreover, thrombin cleaves Val-Pro-Arg-MCA much faster (33-fold) than Phe-Ser-Arg-MCA, which is one of the preferred substrates of trypsin, whereas the activities of neuropsin for these substrates are comparable. In addition, thrombin also exhibits a significant preference for arginine at the P1 position, but no such preference was observed for neuropsin, as described above. These results, together with structural differences of several loops,

verify the unique substrate specificity of neuropsin, even if the P2 preference for proline is analogous to thrombin.

Compared with the subsite preferences on the N-terminal side of the scissile bond, little is known about subsite preferences on the C-terminal side at present. However, a shallow bowl formed by Cys^{42}, Ile^{41}, and Leu^{40} of strand $\beta 3$ seems to provide a hydrophobic S1′ site (Fig. 1*b*). The shape of the substrate-binding surface and the surface electrostatic distribution of neuropsin display several differences in details from other serine proteases. One of the pronounced characteristics is the rim of the S1 pocket, where acidic residues, Asp^{218} and Glu^{149}, expose the side chains to the solvent region. Glu^{97} of the kallikrein loop also is projected from the surface. These characteristics may be related to the specificity that are distinct from those of other proteases. Neuropsin exhibits weak proteolytic activities against gelatin and collagen but effectively cleaves fibronectin, as already mentioned. By changing the extracellular environment, neuropsin may exert its limbic effects.

It is an interesting question whether neuropsin could process NGFβ precursor and form 7 S NGF instead of NGFγ. In 7 S NGF, the active site of NGFγ was occupied by the C-terminal Arg^{118} of the mature NGFβ, as a cleaved product, with extensive interactions of the large nicked kallikrein loop with the C-terminal regions and β-strand of NGFβ. Docking studies suggest that neuropsin would lose most of these interactions although the smaller residues, Thr^{117} and Ala^{116}, of NGFβ could fit to the S2 and S3 sites of neuropsin. In addition, the small cavity of NGFγ for Ala^{116} of NGFβ is missing in neuropsin. Moreover, Lys^{192}, which is located at the rim of the active site of NGFγ and forms hydrogen bonds to main chain carbonyls of Thr^{117} and Lys^{74} of NGFβ, is replaced by Gln^{192} in neuropsin. In 7 S NGF, a zinc ion was located at the interface between NGFγ and NGFα to stabilize the complex. This coordination is also lost when NGFγ is replaced by neuropsin because zinc-coordinated His^{217} and Glu^{222} of NGFγ are replaced by serine and lysine in neuropsin. Taken together, these results suggest that neuropsin is incapable of forming 7 S NGF, even if neuropsin could process the NGFβ precursor. However, this will require further investigation.

In addition to neuropsin, three other serine proteases have been reported to be more highly expressed in the central nervous system than in most peripheral tissues. These include myelencephalon (MSP)-specific protease (7), neurosin (8), and neurotrypsin (6). MSP and neurosin exhibit sequence identities to neuropsin of 48 and 46%, respectively. Neurotrypsin, which is a multidomain serine protease whose expression is most prominent in the cerebral cortex, hippocampus, and amygdala, has a protease domain exhibiting 33% sequence identity to neuropsin. Sequence alignments with neuropsin indicate that these proteases would have different structures of surface loops surrounding the substrate-binding site. Remarkably, loop D of either of these proteases has no *N*-glycosylation site and no inserted residues. This lack of a kallikrein loop would result in their P2 specificities differing from that of neuropsin. Moreover, loop G of MSP and neurosin has no one-residue deletion, which causes significant structural changes of loops G and H forming the S1 pocket. Alternatively, compared with neuropsin, neurotrypsin has a three-residue insertion in loop G and a one-residue deletion in loop H. These differences would endow these other proteases with substrate specificities different from that of neuropsin.

In conclusion, many aspects of neuropsin structure and function reveal that this hippocampal serine protease displays chimeric structural features of trypsin and NGFγ with novel substrate specificity. These findings could give a clue to the structure-based drug design useful in treatment of pathological conditions such as epilepsy and also useful in analyzing the processes of synaptic plasticity.

Acknowledgments—We thank Drs. Ben Bax (Birkbeck College) and S. E. Won Suh (Seoul National University) for providing the coordinates of 7 S NGF and soybean trypsin inhibitor-trypsin complex, respectively; M. Suzuki for data collection at PF; and S. Takayama and J. Tsukamoto for help with the mass spectroscopy and N-terminal analysis.

REFERENCES

1. Monard, D. (1988) *Trends Neurosci.* **11,** 541–544
2. Tsirka, S. E., Gualandris, A., Amaral, D. G., and Strickland, S. (1995) *Nature* **377,** 340–344
3. Liu, Y., Fields, R. D., Festoff, B. W., and Nelson, P. G. (1994) *Proc. Natl. Acad. Sci. U. S. A.* **91,** 10300–10304
4. McGuire, P. G., and Seeds, N. W. (1990) *Neuron* **4,** 633–642
5. Chen, Z.-L., Yoshida, S., Kato, K., Momota, Y., Suzuki, J., Tanaka, T., Ito, J., Nishino, H., Aimoto, S., Kiyama, H., and Shiosaka, S. (1995) *J. Neurosci.* **15,** 5088–5097
6. Gschwend, T. P., Krueger, S. R., Kozlov, S. V., Wolfer, D. P., and Sonderegger, P. (1997) *Mol. Cell. Neurosci.* **9,** 207–219
7. Scarisbrick, I. A., Towner, M. D., and Isackson, P. J. (1997) *J. Neurosci.* **17,** 8156–8168
8. Yamashiro, K., Tsuruoka, N., Kodama, S., Tsujimoto, M., Yamamura, Y., Tanaka, T., Nakazato, H., and Yamagichi, N. (1997) *Biochim. Biophys. Acta* **1350,** 11–14
9. Qian, Z., Gilbert, M. E., Colicos, M. A., Kandel, E. R., and Kuhl, D. (1993) *Nature* **361,** 453–457
10. Okabe, A., Momota, Y., Yoshida, S., Hirata, A., Ito, J., Nishino, H., and Shiosaka, S. (1996) *Brain Res.* **728,** 116–120
11. Momota, Y., Yoshida, S., Ito, J., Shibata, M., Kato, K., Sakurai, K., Matsumoto, K., and Shiosaka, S. (1998) *Eur. J. Neurosci.* **10,** 760–764
12. Akita, H., Matsuyama, T., Iso, H., Sugita, M., and Yoshida, S. (1997) *Brain Res.* **769,** 86–96
13. Kishi, T., Kato, M., Shimizu, T., Kato, K., Matsumoto, K., Yoshida, Y., Shiosaka, S., and Hakoshima, T. (1997) *J. Struct. Biol.* **118,** 248–251
14. Tomiya, N., Awaya, J., Kurono, M., Endo, S., Arata, Y., and Takahashi, N. (1988) *Anal. Biochem.* **171,** 73–90
15. Friedrich, A. (1996) *Trends Glycosci. Glycotech.* **40,** 101–114
16. Otwinowski, Z., and Minor, W. (1996) *Methods Enzymol.* **276,** 307–326
17. Navaza, J. (1994) *Acta Crystallogr. Sec. A* **50,** 157–163
18. Finer-Moore, J. S., Kossiakoff, A. A., Hurley, J. H., Earnest, T., and Stroud, R. M. (1992) *Proteins Struct. Finct.* **12,** 203–222
19. Brunger, A. T., Krukowski, A., and Erickson, J. W. (1990) *Acta Crystallogr. Sec. A* **46,** 585–593
20. Cowtan, K. D., and Main, P. (1996) *Acta Crystallogr. Sec. D* **52,** 43–48
21. Jones, T. A., Zou, J.-Y., Cowan, S. W., and Kjeldgaard, M. (1991) *Acta Crystallogr. Sec. A* **47,** 110–119
22. Laskowski, R. A., MacArthur, M. W., Moss, D. S., and Thornton, J. M. (1993) *J. Appl. Crystallogr.* **26,** 283–291
23. Bax, B., Blundell, T. L., Murray-Rust, J., and McDonald, N. Q. (1997) *Structure* (*Lond.*) **5,** 1275–1285
24. Bode, W., Chen, Z., Bartels, K., Kutzbach, C., Schmidt-Kastner, G., and Bartunik, H. (1983) *J. Mol. Biol.* **164,** 237–282
25. Shimizu, C., Yoshida, S., Shibata, M., Kato, K., Momota, Y., Matsumoto, K., Shiosaka, T., Midorikawa, R., Kamachi, T., Kawabe, A., and Shiosaka, S. (1998) *J. Biol. Chem.* **273,** 11189–11196
26. Timm, D. E. (1997) *Protein Sci.* **6,** 1418–1425
27. Song, H. K., and Suh, S. W. (1998) *J. Mol. Biol.* **275,** 347–363
28. Bode, W., Mayr, I., Baumann, U., Huber, R., Stone, S. R., and Hofsteenge, J. (1989) *EMBO J.* **8,** 3467–3475
29. Hedstrom, L., Perona, J. J., and Rutter, W. J. (1994) *Biochemistry* **33,** 8757–8763